Article published online: 2024-06-04

Original Article

Comparison of hybrid 18F-fluorodeoxyglucose positron emission tomography/magnetic resonance imaging and positron emission tomography/computed tomography for evaluation of peripheral nerve sheath tumors in patients with neurofibromatosis type 1

ABSTRACT

Rapidly enlarging, painful plexiform neurofibromas (PN) in neurofibromatosis type 1 (NF1) patients are at higher risk for harboring a malignant peripheral nerve sheath tumor (MPNST). Fludeoxyglucose (FDG) positron emission tomography/computed tomography (PET/CT) has been used to support more invasive diagnostic and therapeutic interventions. However, PET/CT imparts an untoward radiation hazard to this population with tumor suppressor gene impairment. The use of FDG PET coupled with magnetic resonance imaging (MRI) rather than CT is a safer alternative but its relative diagnostic sensitivity requires verification. Ten patients (6 females, 4 males, mean age 27 years, range 8–54) with NF1 and progressive PN were accrued from our institutional NF Clinic. Indications for PET scanning included increasing pain and/or progressive disability associated with an enlarging PN on serial MRIs. Following a clinically indicated whole-body FDG PET/CT, a contemporaneous PET/MRI was obtained using residual FDG activity with an average time interval of 3–4 h FDG-avid lesions were assessed for both maximum standardized uptake value (SUVmax) from PET/CT and SUVmax from PET/MR and correlation was made between the two parameters. 26 FDG avid lesions were detected on both PET/CT and PET/MR with an accuracy of 100%. SUVmax values ranged from 1.4–10.8 for PET/CT and from 0.2-5.9 for PET/MRI. SUVmax values from both modalities demonstrated positive correlation ($r = 0.45$, $P < 0.001$). PET/MRI radiation dose was significantly lower (53.35% ± 14.37% [$P = 0.006$]). In conclusion, PET/MRI is a feasible alternative to PET/CT in patients with NF1 when screening for the potential occurrence of MPNST. Reduction in radiation exposure approaches 50% compared to PET/CT.

Keywords: Neurofibromatosis type 1, peripheral nerve sheath tumor, positron emission tomography/magnetic resonance

INTRODUCTION

Neurofibromatosis type 1 (NF1) is an autosomal-dominant disease caused by mutations of the NF1 tumor suppressor gene, with an incidence of 1 in 3000.[1-3] Various clinical manifestations occur in NF1, including café au lait spots, Lisch nodules, and skeletal deformities. However, one of the more serious manifestations is the occurrence of plexiform neurofibromas (PNs) thought to arise congenitally and enlarge slowly over time.[4] These tumors may cause significant deformities or clinical morbidity in young children and occasionally undergo malignant transformation in adolescent

Access this article online	
Website: www.wjnm.org	Quick Response Code
DOI: 10.4103/wjnm.WJNM_71_17	

Roy A. Raad, Shailee Lala, Jeffrey C. Allen[1], James Babb, Carole Wind Mitchell, Ana M. Franceschi, Kaleb Yohay, Kent P. Friedman

Departments of Radiology and [1]Pediatrics and Neurology, NYU School of Medicine, New York, NY 10016, USA

Address for correspondence: Dr. Roy A. Raad, Department of Radiology, NYU School of Medicine, 550 First Avenue, New York, NY 10016, USA.
E-mail: royraad@gmail.com

How to cite this article: Raad RA, Lala S, Allen JC, Babb J, Mitchell CW, Franceschi AM, *et al.* Comparison of hybrid 18F-fluorodeoxyglucose positron emission tomography/magnetic resonance imaging and positron emission tomography/computed tomography for evaluation of peripheral nerve sheath tumors in patients with neurofibromatosis type 1. World J Nucl Med 2018;17:241-8.

or adulthood. The lifetime risk of developing a malignant peripheral nerve sheath tumors (MPNSTs) ranges from 8% to 13%.[5,6] Early signs of malignant transformation include relentless pain, rapid enlargement, changes in consistency on physical examination, and new/worsening neurologic symptoms.[7] Curative treatment requires total surgical resection so early diagnosis is essential.

Accurate differentiation between benign PNs and MPNSTs using anatomic cross-sectional imaging modalities can be challenging. Although several magnetic resonance imaging (MRI) features have been described as favoring MPNSTs, such as ill-defined margins, irregular enhancement, intratumoral lobulation, and perilesional edema, utilization of MRI by itself has proven to be insufficiently accurate, with reported sensitivity and specificity of 61% and 90%, respectively.[8,9] Whole-body MRI has also been used to assess disease burden in NF1 patients, without proven accuracy in differentiating benign from malignant entities.[9] Accurate histologic assessment of benign and malignant lesions can also be difficult, often due to tissue sampling error, with up to 20% of lesions having ambiguous histologic features which may lead to repeated diagnostic procedures.[10,11]

Currently, 18F-fluorodeoxyglucose (^{18}F-FDG) positron emission tomography/computed tomography (PET/CT) is considered a well-recognized sensitive imaging modality for detection of MPNSTs.[1,8,12-15] Moreover, 18F-FDG PET/CT may be useful in preoperative tumor staging, guiding biopsies to the region of highest diagnostic yield within the tumor or providing incentives to radically resect tumors with worrisome imaging features, if feasible.[16-18] Maximum standardized uptake value (SUVmax) is the most accepted PET/CT parameter used to distinguish between benign PNs and MPNSTs in NF1 patients. Despite the range of SUVmax values that have been associated with malignant tumors (1.8–7.0),[1,19] the most widely used cutoff value is a SUVmax of 3.5. There is some hesitation to perform sequential PET/CT scans in sensitive populations such as children and/or those with tumor suppressor gene disorders such as NF1 because each scan imparts a relatively high-radiation total body exposure from the combined impact of the CT and radiotracer.[20,21] Patients with NF1 are at increased risk of developing radiation-induced malignancies, most commonly MPNSTs,[22,23] as well as few reported additional malignancies such as high-grade brain gliomas.[24]

The recent introduction of whole-body combined PET and MRI systems (PET/MRI) offers the capability of combining the high-resolution and functional information of MRI and the metabolic activity information of PET, to accurately assess tumors in NF1 patients, as well as differentiate between benign PNs and MPNSTs. Compared to PET/CT, PET/MRI offers superior anatomic contrast resolution, at a reduced radiation exposure since MRI does not involve ionizing radiation for image acquisition.

Hence, the purpose of this study was to compare the accuracy of contemporaneously acquired PET/MRI for detection and quantitative evaluation of benign PNs and MPNSTs in patients with NF1, using PET/CT as a reference standard. The secondary aim of this study was to compare radiation dose in PET/MRI versus diagnostic PET/CT.

MATERIALS AND METHODS

PET/MRI data were acquired as a part of a prospective Health Insurance Portability, and Accountability Act compliant Institutional Review Board approved study comparing PET/MRI to PET/CT. All patients signed a written informed consent for undergoing a whole-body PET/MRI immediately after their clinically indicated PET/CT. Indications for PET scanning included increasing pain and/or disability associated with a previously identified and enlarging PN on serial prior MRIs. FDG was injected before the PET/CT, and PET/MRI data were subsequently acquired following the completion of the PET/CT scanning using residual radiotracer activity. The average differential in timing of the PET/CT versus PET/MRI was 3–4 h and the PET/CT was always performed first.

Between January 2013 and July 2013, 10 patients (6 females, 4 males; mean age 27 years, range 8–54 years) with NF1 and progressive PNs were accrued from our institutional Comprehensive NF Clinic. The indications for PET imaging included worsening pain (3/10 patients) and enlarging mass (7/10 patients), either clinically or on prior cross-sectional imaging.

Positron emission tomography/computed tomography examination

All patients fasted for at least 4 h before the examination. When applicable, insulin was discontinued 6 h before the examination, with the target blood glucose level verified to be <11.1 mmol/L (200 mg/dL) in all patients. All patients received oral barium sulfate, whereas none of them received intravenous (IV) iodinated contrast. The administered FDG dose was 555 MBq (15 mCi) for most patients, apart from the three pediatric patients who received a lower weight-based dose of 3.7–5.2 MBq/kg (0.1–0.14 mCi/kg).[25] Therefore, the injected FDG dose range was 111–558.7 MBq (3.0–15.1 mCi), mean dose was 444 MBq (12.0 mCi), with a standard deviation of ±173.9 MBq (4.7 mCi). After administration of an IV injection of FDG, patients were required to sit quietly in a

dimly lit room for approximately 45 min and were asked to void before imaging. The range of PET/CT uptake times was 51–97 min with mean uptake time of 68 min and a standard deviation of ± 15 min. Images were then obtained from the vertex of the skull to the toes.

The PET/CT examination was performed on a Biograph mCT unit (Siemens Healthcare, Knoxville, USA). Acquisition parameters for CT include peak voltage of 120 kVp, Care Dose4D (Siemens Healthcare, Erlangen, Germany) modulation with a reference tube current of 95 mAs for nonenhanced studies and 140 mAs for IV contrast material-enhanced studies, rotation time of 0.3–0.5 s, and collimation of 16 mm × 1.2 mm. A pediatric-tailored protocol was used for the three pediatric patients, including Care Dose4D (Siemens Healthcare, Erlangen, Germany) modulation with a reference tube current of 25 mAs for patients <100 lbs and 60 mAs for patients weighing more than 100 lbs.

Subsequently, the PET data were acquired with an imaging time of 2-3 min per bed depending on patient weight and uptake time. PET data were reconstructed using the manufacturer-provided standard software with a three-dimensional ordinary Poisson ordered subset expectation maximization algorithm, two iterations, 21 subsets, and 2-mm Gaussian filter (image matrix, 168 × 168; voxel size, 1.78 mm × 1.78 mm × 2 mm). The manufacturer reported sensitivity of the Biograph PET/CT system is 8.5 kcps/MBq. The attenuation correction was based on the CT data.

Positron emission tomography/magnetic resonance imaging examination

PET/MR imaging was performed using an integrated PET/MR system (Biograph mMR; Siemens Healthcare), which acquires simultaneous PET and MRI data with a 3.0-T magnet.

PET/MR imaging was initiated on average 214.1 min after tracer injection (range 170-248 min, standard deviation ± 27 min), however, patients were not re-injected with FDG before the start of the PET/MR examination. Residual ^{18}F-FDG from the earlier PET/CT injection was utilized for PET/MR examination. Of note, the two examinations were performed between 106 and 187 min apart. The mean time interval between the studies was 146 min, with a standard deviation of ± 28.5 min. The long delay between the PET/CT and PET/MR studies is attributed to the location of the two scanners in two different sites at our institution. Eight of the 10 patients received additional gadolinium contrast intravenously. For the two patients who did not receive gadolinium, no sufficient information regarding their renal function was available at the time of the scan. PET and MR data were acquired simultaneously.

For each bed position, an approximately 20-s breath-hold T1-weighted Dixon gradient echo sequence in the coronal plane was acquired first for attenuation correction. This was used to generate an attenuation map, as described previously[26,27] with an MR-based segmentation method, separating fat, soft tissue, lung, and background attenuation. Immediately thereafter, the following MR sequences were performed in the transaxial plane simultaneously with PET scanning in free-breathing through multiple stations: T1-weighted gradient echo imaging with radial stack-of-stars trajectory (STAR VIBE, Siemens HealthCare, Germany),[28] axial and coronal T2-weighted short T1 inversion recovery (STIR). STAR VIBE was acquired with the following parameters: repetition time TR 4.5 ms/echo time TE 2 ms; section thickness, 2.5 mm; flip angle, 12°; 80 axial slices; bandwidth, 400 Hz per pixel; voxel size, 1.4 mm × 1.4 mm × 2.5 mm; and quick fat-saturation mode. The parameters for the STIR sequence were as follows TR/TE 5000/56 ms; slice thickness 5 mm; flip angle 135°; 30 axial slices.

The acquired PET sinogram was reconstructed using the three-dimensional ordinary Poisson ordered-subset expectation maximization algorithm (four iterations, 21 subsets). The manufacturer reported sensitivity of the mMR system is 13.2 kcps/MBq.

Image interpretation

PET/CT – One radiologist with 6 years of experience (including fellowship training in thoracic and PET imaging) interpreted the PET/CT examination. PET/CT images were independently interpreted using the MIM 6.2 fusion viewer (MIM Software, Cleveland, Ohio, USA). The reader noted the presence of any soft tissue masses, their size, location in the body, and presence or absence of any identifiable FDG uptake above background activity. Detected soft tissue masses were annotated and images were then saved. This PET/CT interpretation was considered to be the reference standard.

PET/MR – Subsequent to the PET/CT reading, the reader independently interpreted the PET/MR images with delay of at least 2 weeks between the PET/CT and PET/MR reading sessions to minimize recall bias. The PET, STAR VIBE, and STIR images were interpreted together using the XD3 software (version 3.6; Mirada Medical, Oxford, England). Attenuation-corrected PET images were fused to both STAR VIBE and STIR images for this interpretation. Presence, size, location, and FDG avidity of soft tissue masses were noted for PET/MR data sets. All masses were annotated and the images were saved. For the 8 patients who received gadolinium, both the pre- and post-contrast sequences were evaluated.

Quantitative analysis

The reader measured the SUVmax of the target lesion and any large secondary masses on the PET images for both PET/CT and PET/MRI, by manually measuring 3D volumes of interest on the MIM fusion viewer.

Radiation dose

Effective dose ED due to the PET scan was calculated as follows:

- ED^{PET} (mSv) = AD^{FDG} (MBq) × 0.017(mSv/MBq)

AD is the administered dose and 0.017 mSv/MBq is the whole body ED coefficient recommended by Brix *et al*.,[29] based on the International Commission of Radiation Protection ICRP publication.[30] ED due to the CT portion of the examination was estimated according to the method described by Huda *et al*.[31] where ED is determined by multiplying the CT dose length product DLP by the ED/DLP ratio. The ED/DLP ratio for whole body scans is reported as 15.4 uSv/mGy at 120 kV,[32] based on ICRP 103 tissue weighting factors.[30] The equation for CT ED is below:

- ED^{CT} (mSv) = DLP (mGy-cm) × 15.4 (uSv/mGy-cm)/ 1000 (mSv/uSv)

  Equations for PET/CT ED and PET/MRI ED are below:
- $ED^{PET/CT} = ED^{PET} + ED^{CT}$
- $ED^{PET/MRI} = ED^{PET}$.

Statistical methods

The association between SUVmax from PET/CT and PET/MRI was characterized in terms of the Pearson correlation coefficient and the mixed model regression line to predict SUVmax from PET/CT as a function of SUVmax from PET/MRI. To account for the lack of statistical independence among values derived for lesions within the same patient, mixed model analysis assumed observations to be symmetrically correlated when acquired from the same patient and to be independent when acquired from different patients. The normality assumption underlying the regression analysis was validated by a Schapiro–Wilks test applied to the model residuals. Literal agreement between the SUVmax values from PET/CT and PET/MRI was assessed in terms of the concordance correlation. An exact paired-sample Wilcoxon signed rank test was used to compare the radiation exposures associated with PET/CT and PET/MRI. All statistical tests were conducted at the two-sided 5% significance level using SAS 9.3 software (SAS Institute, Cary, NC, USA).

RESULTS

The study cohort demographics including patient age, gender, lesion location, and SUV values from both PET/CT and PET/MRI are described in Table 1. A total of 26 FDG avid soft tissue lesions were detected on the (reference standard) whole-body PET/CT, all of which were identified on the whole-body PET/MRI, with a sensitivity of 100%. No additional FDG avid lesions were identified on the PET/MRI and not on the PET/CT [Figure 1]. SUVmax values for the lesions detected on PET/CT (SUVmax PET/CT) ranged between 1.4 and 10.8 (mean value 3.9), where the SUVmax values for the lesions detected on PET/MRI (SUVmax PET/MRI) ranged between 0.2 and 5.9 (mean value 2.7) [Figures 2 and 3]. There was a moderate correlation between SUVmax from PET/CT and PET/MR, with a Pearson correlation of r = 0.45 that the mixed model analysis revealed to be statistically significant ($P = 0.009$). The regression line to predict SUVmax from PET/CT as a function of SUVmax from PET/MR is depicted in Figure 4 and is given by the equation:

Predicted SUVmax from PET-CT = 1.884 + 0.72 × SUVmax from PET-MR.

The intercept being significantly different from zero ($P = 0.047$) and the slope being significantly different from unity ($P < 0.001$) implies that the use of SUVmax from PET/MRI to estimate SUVmax from PET/CT is associated with significant additive and multiplicative bias, respectively. In terms of literal agreement, the concordance correlation was 0.36, which is typically interpreted as an indication of poor agreement. The SUVmax values from the PET/CT procedures were greater than those from the same lesions on PET/MRI for the majority of the subjects (19/26 lesions), probably reflecting the 3–4 h time difference.

Concerning the radiation doses, ED^{PET} values, which are equivalent to the $ED^{PET/MRI}$ values, ranged between 1.9 and 9.5 mSv with a mean value of 7.6 mSv. The ED^{CT} values ranged between 4.3 and 17.0 mSv with a mean value of 8.8 mSv, whereas the $ED^{PET/CT}$ values ranged between 7.2 and 26.4 mSv with a mean value of 16.3. The mean ± standard deviation (median) of the radiation dose was 16.34 ± 6.21 (14.78) mSv for PET/CT and 7.57 ± 2.94 (9.35) mSv for PET/MRI. The Wilcoxon test showed the median dose to be significantly lower for PET/MRI than for PET/CT ($P = 0.006$). A 95% confidence interval (CI) for the median reduction in dose associated with PET/MRI relative to PET/CT extends from 5.26-12.20 mSv. The within-subject percentage reduction in dose for PET/MR relative to PET/CT was computed as 100% × ($ED^{CT}/ED^{PET/CT}$). The mean ± standard deviation (median) of the percentage reduction in radiation dose was 53.35% ±14.37% (52.17%). The Wilcoxon test showed the median percentage reduction in dose to be significantly >0 ($P = 0.006$). A 95% CI for the mean percentage reduction in dose extends from 43.1% to 63.6% and a 95% CI for the median percentage reduction in dose extends from 42.3% to 63.8%.

Table 1: Study cohort demographics including patient age, gender, lesion location, and Standardized uptake value values from both positron emission tomography/computed tomography and positron emission tomography/magnetic resonance imaging

Patient number	Sex	Age	Lesion Location	SUV_{max} PET-CT	SUV_{max} PET-MR
1	Female	32	Retroperitoneum	5.2	5.7
			Left pleural space	3.6	4.2
			Pelvis	5.0	5.9
2	Female	20	Right axilla	7.3	1.0
			Right upper extremity	2.7	0.2
			Pelvis	2.8	1.8
			Left buttock	5.8	4.1
			Pelvis	2.1	1.3
3	Male	47	Right paraspinal	4.5	5.3
			Posterior neck subcutaneous	2.2	1.1
			Upper back, subcutaneous	1.9	0.8
4	Male	8	Retroperitoneum	2.1	3.3
			Right thigh	1.4	2.2
5	Female	20	Left upper quadrant abdominal	10.8	2.6
			Left anterior thigh	3.3	0.4
			Left anterior thigh	3.4	0.4
			Left anterior thigh	1.6	0.7
6	Female	30	Mesenteric	8.3	5.5
			Right suprarenal	3.4	2.8
7	Female	54	Right upper extremity	4.4	4.1
8	Female	27	Right lower extremity	5.1	3.5
9	Male	23	Left posterior thigh	4.6	4.0
			Right anterior thigh	2.8	3.0
			Left distal femur	2.1	1.6
			Right anterior thigh	3.3	2.7
10	Male	9	Upper back, subcutaneous	1.7	1.2

SUV_{max}: Maximum standardized uptake value; PET-CT: Positron emission tomography-computed tomography; PET-MR: Positron emission tomography-magnetic resonance

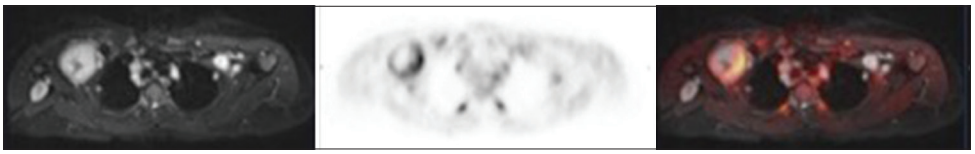

Figure 1: Axial short T1 inversion recovery (left), positron emission tomography (center), and fused post hoc (right) images demonstrate a hyperintense right axillary mass with central cystic component, intense peripheral fludeoxyglucose uptake (maximum standardized uptake value 5.7). Tumor was malignant at surgery

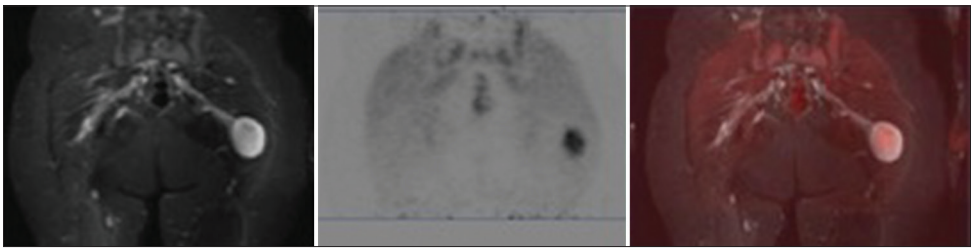

Figure 2: Coronal short T1 inversion recovery (left), positron emission tomography (center), and fused post hoc (right) images of a left gluteus muscle mass demonstrating high T2 signal intensity and mild fludeoxyglucose uptake (maximum standardized uptake value = 3.7). Imaging findings were consistent with a benign or atypical plexiform neurofibroma

DISCUSSION

In this study, we compared whole-body PET/MRI to the reference standard PET/CT for evaluation of peripheral nerve sheath tumors in patients with NF1 undergoing a clinically indicated whole-body PET/CT. Contemporaneously acquired hybrid PET/MRI demonstrated a sensitivity similar to that of PET/CT for detection of FDG avid soft tissue

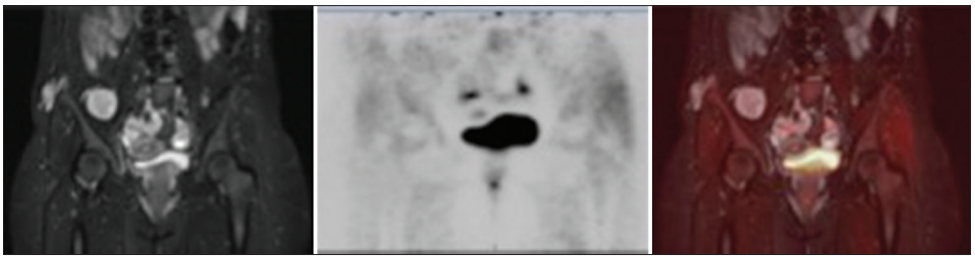

Figure 3: Coronal short T1 inversion recovery (left), positron emission tomography (center), and fused post hoc images (right) of right gluteus maximus and right iliacus lesions also demonstrating high T2 signal intensity and mild flurodeoxyglucose uptake (maximum standardized uptake value = 3.3 and 2.1 respectively). Imaging findings were consistent with benign plexiform neurofibromas

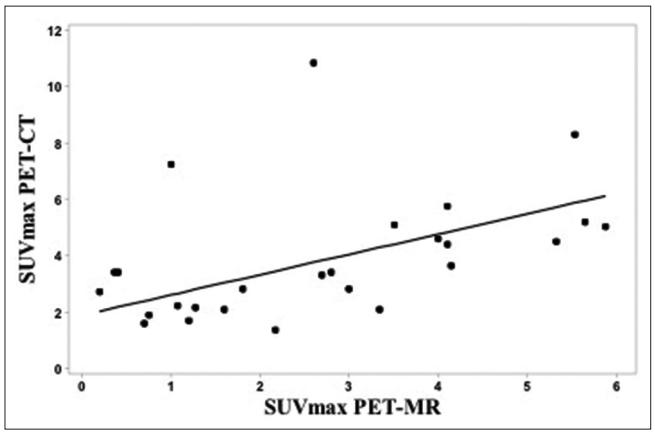

Figure 4: Scatter plot of maximum standardized uptake value from positron emission tomography/computed tomography versus maximum standardized uptake value from positron emission tomography/magnetic resonance imaging with the mixed model regression line to predict maximum standardized uptake value from positron emission tomography/computed tomography as a function of maximum standardized uptake value from positron emission tomography/magnetic resonance imaging

lesions in these patients. There was a significant and strong positive correlation between SUVmax values measured on PET/CT and those measured on PET/MRI for the target and secondary soft tissue lesions. The majority of the lesions (19/26) detected on PET/MRI demonstrated lower SUVmax values compared to those detected on PET/CT, which is in concordance with previously reported results in the literature which found apparent underestimation of SUV values on PET/MRI when compared to PET/CT.[33-35] The reason for this is not clear, however, may be possibly attributed to tracer washout since PET/MRI was obtained at a 2–3 h later time point following FDG injection compared to PET/CT. Regarding the remaining 7 lesions that showed higher SUVmax values on PET/MR compared to PET/CT, the reason was also unclear. This may be due to progressive accumulation of the tracer within lesions, and further research is needed to demonstrate whether this pattern is more likely to occur in malignant lesions.

The significant positive correlation between SUVmax values measured on PET/CT and PET/MRI in our patient cohort has been reproduced in several recent studies for a variety of organs and disease processes,[33-37] such as for lymphoma[35,36] and lung cancer.[37] The value of 18F-FDG PET/CT and MRI as separate imaging modalities for assessment of PNs and malignant transformation to MPNSTs in NF1 patients is well established, however, according to our knowledge, this is, the first study assessing the role of hybrid simultaneously acquired PET/MRI in NF1 patients. MRI is usually performed for assessment of tumor burden and routine surveillance in NF1 patients, including both whole body imaging and dedicated imaging of the area of concern. On the other hand, whole-body PET/CT is usually indicated for evaluation of malignant transformation to MPNSTs based on suspicious clinical features such as rapid enlargement or worsening pain/neuropathy, as well as a demonstration of suspicious findings on initial MRI. Despite the wide variation and lack of consensus regarding the cutoff SUVmax for suggesting malignant transformation, 18F-FDG PET/CT is a highly sensitive and specific modality for detection of MPNSTs, with reported sensitivity up to 100% and specificity of 77%–95%.[38]

Naturally, the radiation dose from PET/MRI will be lower than that of PET/CT, and in our study, we calculated a significant dose reduction. NF1 patients with tumor suppressor gene impairment are at increased risk of developing radiation-induced malignancies,[22-24] hence "As Low As Reasonably Achievable" radiation doses are particularly attractive for this and other sensitive populations such as children, especially given the likelihood of the need for repeated imaging in these patients. The CT examination performed part of the PET/CT at our institution is of diagnostic quality; therefore, our estimated radiation dose savings may be higher compared to other institutions.

Results of our study demonstrated similar sensitivity and strong correlation between PET/CT and PET/MRI, suggesting that PET/MRI is a feasible alternative imaging modality for assessment of potential MPNSTs in NF1 patients, at a reduced radiation dose compared to PET/CT. In addition to the superior contrast resolution of MRI compared to CT, PET/MRI offers additional sequences that can potentially

be used for noninvasive differentiation of benign from malignant lesions, such as DWI, perfusion analysis on dynamic contrast-enhanced MRI, and MR spectroscopy MRS,[36,39] all of which require further investigation.

Limitations of our study included a small number of patients and detected lesions, as well as heterogeneous population, including patients of different age groups and extent of disease, which may have affected SUV measurements. The use of a single reader is another potential limitation, however, this is unlikely to be significant given the similar sensitivity of lesion detection demonstrated on PET/CT and PET/MRI, as well as the quantitative objective nature of SUVmax measurements, which is unlikely to vary among different readers. In addition, IV contrast was administered for most PET/MRI examinations but not for PET/CT examinations. Diffusion-weighted imaging DWI is a potentially important parameter for distinguishing malignant from benign peripheral nerve sheath tumors.[40] Although DWI was included in our PET/MR protocol, the apparent diffusion coefficient ADC values were not included in our study secondary to significant limitations of quantification, mainly due to significant patient motion artifacts. This is, however, a potentially significant component of PET/MR imaging, which merits further investigation, potentially using shorter imaging times and patient sedation. Another limitation is the lack of standardization of time points for imaging, specifically the longer uptake times for PET/MRI compared to PET/CT attributed to the presence of the PET/MRI scanner at a different location, which may have affected SUV measurements, however, unlikely to have affected lesion detection given the similar sensitivity demonstrated for both modalities. Future investigations using earlier and more standardized time points after FDG injection are required for further validation of PET/MRI in these patients. Concerning radiation dose calculation, the method we used is based on a constant 120 kV X-ray tube output, whereas our CT protocol makes use of current modulation, which may have led to overestimation of dose calculations, though not by a large amount as shown by van Straten *et al*.[41] Finally, histologic correlation was not available for the majority of the detected lesions, an advantage that can be used in future investigations to further validate the utility of PET/MRI.

CONCLUSION

Whole-body hybrid PET/MRI is a viable alternative for evaluation of the potential occurrence of MPNSTs in NF1 patients, with sensitivity similar to that of PET/CT. Furthermore, dose reduction with PET/MR approaches 50% compared to PET/CT, a vital concern in this patient population with tumor suppressor gene impairment. We currently perform PET/MRI in NF1 patients with evolving or increasingly painful preexisting PNs, to monitor for early signs of malignant transformation.

Financial support and sponsorship

Nil.

Conflicts of interest

There are no conflicts of interest.

REFERENCES

1. Ferner RE, Golding JF, Smith M, Calonje E, Jan W, Sanjayanathan V, *et al*. [18F]2-fluoro-2-deoxy-D-glucose positron emission tomography (FDG PET) as a diagnostic tool for neurofibromatosis 1 (NF1) associated malignant peripheral nerve sheath tumours (MPNSTs): A long-term clinical study. Ann Oncol 2008;19:390-4.
2. Korf BR. Clinical features and pathobiology of neurofibromatosis 1. J Child Neurol 2002;17:573-7.
3. Thomson SA, Fishbein L, Wallace MR. NF1 mutations and molecular testing. J Child Neurol 2002;17:555-61.
4. Mautner VF, Asuagbor FA, Dombi E, Fünsterer C, Kluwe L, Wenzel R, *et al*. Assessment of benign tumor burden by whole-body MRI in patients with neurofibromatosis 1. Neuro Oncol 2008;10:593-8.
5. Nguyen R, Jett K, Harris GJ, Cai W, Friedman JM, Mautner VF, *et al*. Benign whole body tumor volume is a risk factor for malignant peripheral nerve sheath tumors in neurofibromatosis type 1. J Neurooncol 2014;116:307-13.
6. Evans DG, Baser ME, McGaughran J, Sharif S, Howard E, Moran A, *et al*. Malignant peripheral nerve sheath tumours in neurofibromatosis 1. J Med Genet 2002;39:311-4.
7. Ferner RE, Gutmann DH. International consensus statement on malignant peripheral nerve sheath tumors in neurofibromatosis. Cancer Res 2002;62:1573-7.
8. Tsai LL, Drubach L, Fahey F, Irons M, Voss S, Ullrich NJ, *et al*. [18F]-fluorodeoxyglucose positron emission tomography in children with neurofibromatosis type 1 and plexiform neurofibromas: Correlation with malignant transformation. J Neurooncol 2012;108:469-75.
9. Derlin T, Tornquist K, Münster S, Apostolova I, Hagel C, Friedrich RE, *et al*. Comparative effectiveness of 18F-FDG PET/CT versus whole-body MRI for detection of malignant peripheral nerve sheath tumors in neurofibromatosis type 1. Clin Nucl Med 2013;38:e19-25.
10. Woodruff JM. Pathology of tumors of the peripheral nerve sheath in type 1 neurofibromatosis. Am J Med Genet 1999;89:23-30.
11. Spurlock G, Knight SJ, Thomas N, Kiehl TR, Guha A, Upadhyaya M, *et al*. Molecular evolution of a neurofibroma to malignant peripheral nerve sheath tumor (MPNST) in an NF1 patient: Correlation between histopathological, clinical and molecular findings. J Cancer Res Clin Oncol 2010;136:1869-80.
12. Treglia G, Taralli S, Bertagna F, Salsano M, Muoio B, Novellis P, *et al*. Usefulness of whole-body fluorine-18-fluorodeoxyglucose positron emission tomography in patients with neurofibromatosis type 1: A systematic review. Radiol Res Pract 2012;2012:431029.
13. Karabatsou K, Kiehl TR, Wilson DM, Hendler A, Guha A. Potential role of 18fluorodeoxyglucose-positron emission tomography/computed tomography in differentiating benign neurofibroma from malignant peripheral nerve sheath tumor associated with neurofibromatosis 1. Neurosurgery 2009;65:A160-70.
14. Warbey VS, Ferner RE, Dunn JT, Calonje E, O'Doherty MJ. [18F]FDG

PET/CT in the diagnosis of malignant peripheral nerve sheath tumours in neurofibromatosis type-1. Eur J Nucl Med Mol Imaging 2009;36:751-7.
15. Bredella MA, Torriani M, Hornicek F, Ouellette HA, Plamer WE, Williams Z, *et al.* Value of PET in the assessment of patients with neurofibromatosis type 1. AJR Am J Roentgenol 2007;189:928-35.
16. Wegner EA, Barrington SF, Kingston JE, Robinson RO, Ferner RE, Taj M, *et al.* The impact of PET scanning on management of paediatric oncology patients. Eur J Nucl Med Mol Imaging 2005;32:23-30.
17. Brenner W, Friedrich RE, Gawad KA, Hagel C, von Deimling A, de Wit M, *et al.* Prognostic relevance of FDG PET in patients with neurofibromatosis type-1 and malignant peripheral nerve sheath tumours. Eur J Nucl Med Mol Imaging 2006;33:428-32.
18. Fisher MJ, Basu S, Dombi E, Yu JQ, Widemann BC, Pollock AN, *et al*. The role of [18F]-fluorodeoxyglucose positron emission tomography in predicting plexiform neurofibroma progression. J Neurooncol. 2008;87:165-71.
19. Cardona S, Schwarzbach M, Hinz U, Dimitrakopoulou-Strauss A, Attigah N, Mechtersheimer Section Sign G, *et al*. Evaluation of F18-deoxyglucose positron emission tomography (FDG-PET) to assess the nature of neurogenic tumours. Eur J Surg Oncol 2003;29:536-41.
20. Huang B, Law MW, Khong PL. Whole-body PET/CT scanning: Estimation of radiation dose and cancer risk. Radiology 2009;251:166-74.
21. Brix G, Lechel U, Glatting G, Ziegler SI, Münzing W, Müller SP, *et al.* Radiation exposure of patients undergoing whole-body dual-modality 18F-FDG PET/CT examinations. J Nucl Med 2005;46:608-13.
22. Sharif S, Ferner R, Birch JM, Gillespie JE, Gattamaneni HR, Baser ME, *et al.* Second primary tumors in neurofibromatosis 1 patients treated for optic glioma: Substantial risks after radiotherapy. J Clin Oncol 2006;24:2570-5.
23. Ducatman BS, Scheithauer BW, Piepgras DG, Reiman HM, Ilstrup DM. Malignant peripheral nerve sheath tumors. A clinicopathologic study of 120 cases. Cancer 1986;57:2006-21.
24. Madden JR, Rush SZ, Stence N, Foreman NK, Liu AK. Radiation-induced gliomas in 2 pediatric patients with neurofibromatosis type 1: Case study and summary of the literature. J Pediatr Hematol Oncol 2014;36:e105-8.
25. Gelfand MJ, Parisi MT, Treves ST, Pediatric Nuclear Medicine Dose Reduction Workgroup. Pediatric radiopharmaceutical administered doses: 2010 North American consensus guidelines. J Nucl Med 2011;52:318-22.
26. Chandarana H, Heacock L, Rakheja R, DeMello LR, Bonavita J, Block TK, *et al.* Pulmonary nodules in patients with primary malignancy: Comparison of hybrid PET/MR and PET/CT imaging. Radiology 2013;268:874-81.
27. Rakheja R, DeMello L, Chandarana H, Glielmi C, Geppert C, Faul D, *et al.* Comparison of the accuracy of PET/CT and PET/MRI spatial registration of multiple metastatic lesions. AJR Am J Roentgenol 2013;201:1120-3.
28. Chandarana H, Block TK, Rosenkrantz AB, Lim RP, Kim D, Mossa DJ, *et al.* Free-breathing radial 3D fat-suppressed T1-weighted gradient echo sequence: A viable alternative for contrast-enhanced liver imaging in patients unable to suspend respiration. Invest Radiol 2011;46:648-53.
29. Brix G, Nosske D, Lechel U. Radiation exposure of patients undergoing whole-body FDG-PET/CT examinations: An update pursuant to the new ICRP recommendations. Nuklearmedizin 2014;53:217-20.
30. The 2007 recommendations of the international commission on radiological protection. ICRP publication 103. Ann ICRP 2007;37:1-332.
31. Huda W, Ogden KM, Khorasani MR. Converting dose-length product to effective dose at CT. Radiology 2008;248:995-1003.
32. Huda W, Magill D, He W. CT effective dose per dose length product using ICRP 103 weighting factors. Med Phys 2011;38:1261-5.
33. Drzezga A, Souvatzoglou M, Eiber M, Beer AJ, Fürst S, Martinez-Möller A, *et al.* First clinical experience with integrated whole-body PET/MR: Comparison to PET/CT in patients with oncologic diagnoses. J Nucl Med 2012;53:845-55.
34. Wiesmüller M, Quick HH, Navalpakkam B, Lell MM, Uder M, Ritt P, *et al.* Comparison of lesion detection and quantitation of tracer uptake between PET from a simultaneously acquiring whole-body PET/MR hybrid scanner and PET from PET/CT. Eur J Nucl Med Mol Imaging 2013;40:12-21.
35. Sher AC, Seghers V, Paldino MJ, Dodge C, Krishnamurthy R, Krishnamurthy R, *et al.* Assessment of sequential PET/MRI in comparison with PET/CT of pediatric lymphoma: A Prospective study. AJR Am J Roentgenol 2016;206:623-31.
36. Heacock L, Weissbrot J, Raad R, Campbell N, Friedman KP, Ponzo F, *et al.* PET/MRI for the evaluation of patients with lymphoma: Initial observations. AJR Am J Roentgenol 2015;204:842-8.
37. Heusch P, Buchbender C, Köhler J, Nensa F, Gauler T, Gomez B, *et al.* Thoracic staging in lung cancer: Prospective comparison of 18F-FDG PET/MR imaging and 18F-FDG PET/CT. J Nucl Med 2014;55:373-8.
38. Salamon J, Mautner VF, Adam G, Derlin T. Multimodal imaging in neurofibromatosis type 1-associated nerve sheath tumors. Rofo 2015;187:1084-92.
39. Fayad LM, Wang X, Blakeley JO, Durand DJ, Jacobs MA, Demehri S, *et al.* Characterization of peripheral nerve sheath tumors with 3T proton MR spectroscopy. AJNR Am J Neuroradiol 2014;35:1035-41.
40. Demehri S, Belzberg A, Blakeley J, Fayad LM. Conventional and functional MR imaging of peripheral nerve sheath tumors: Initial experience. AJNR Am J Neuroradiol 2014;35:1615-20.
41. van Straten M, Deak P, Shrimpton PC, Kalender WA. The effect of angular and longitudinal tube current modulations on the estimation of organ and effective doses in x-ray computed tomography. Med Phys 2009;36:4881-9.